Synthesis and Structure of Platinum–Tungsten and –Molybdenum Heterodinuclear Complexes with Alkyl and Aryl Ligands: Mechanistic Study of the Migration of Alkyl and Aryl Groups from Platinum to Tungsten and Molybdenum

Atsushi Fukuoka, Takanori Sadashima, Isao Endo, Nobutoshi Ohashi, Yutaka Kambara, Takeshi Sugiura, Kunio Miki,[†,‡] Nobutami Kasai,[†] and Sanshiro Komiya*

Department of Applied Chemistry, Tokyo University of Agriculture and Technology, 2-24-16, Nakacho, Koganei, Tokyo 184, Japan, and Department of Applied Chemistry, Osaka University, Yamadaoka, Suita, Osaka 565, Japan

Received January 3, 1994[⊗]

A series of heterodinuclear platinum–tungsten and –molybdenum complexes (cod)RPt–M(CP)(CO)$_3$ has been prepared by the metathetical reactions: M = W, CP = Cp, R = Me (**1a**), Et (**1b**), Ph (**1c**), 2-MeC$_6$H$_4$ (**1d**), 4-MeC$_6$H$_4$ (**1e**), 2,6-(Me)$_2$C$_6$H$_3$ (**1f**), 4-MeOC$_6$H$_4$ (**1g**), C$_6$F$_5$ (**1h**), 4-FC$_6$H$_4$ (**1i**), 4-ClC$_6$H$_4$ (**1j**); M = W, CP = C$_5$H$_4$Me, R = Me (**2a**), Ph (**2b**), M = W, Cp = C$_5$H$_4$COOMe, R = Me (**3a**), Ph (**3b**); M = Mo, CP = Cp, R = Me (**4a**), Ph (**4b**), 2-MeC$_6$H$_4$ (**4c**). (cod)PhPt–MoCp(CO)$_3$ (**4b**) crystallizes in the monoclinic system in space group $P2_1/n$ with a = 14.291(5) Å, b = 12.738(3) Å, c = 11.988(4) Å, β = 112.01(3)°, Z = 4, R = 0.057 (R_w = 0.078), based on 3719 reflections with $|F_o| > 3\sigma(|F_o|)$. **4b** is isostructural to the Pt–W analogue **1c** determined previously and the geometry at Pt is square planar, where the Pt–Mo bond distance is 2.832(1) Å. The alkyl and aryl ligands on Pt migrate to the other metal in thermolysis in C$_6$D$_6$ at 70 °C. The migration is accelerated by CO as well as by PPh$_3$ or P(OPh)$_3$. In contrast, the reaction of **1a** with PMe$_3$ does not result in the methyl migration but affords [PtMe(PMe$_3$)$_3$]$^+$ [WCp(CO)$_3$]$^-$ (**5**). Moreover, the migration is accelerated by acrylonitrile and the rate is first order in the concentration of acrylonitrile, but further addition of COD retards the rate of migration. From kinetic investigation, the mechanism of the methyl migration for **1a** is proposed. In the mechanism, acrylonitrile coordinates to **1a** to form a five-coordinated intermediate (**6**), and **6** dissociates COD to form a three-coordinated intermediate (**7**). MeWCp(CO)$_3$ (**8**) is produced from **1a**, **6**, and **7**.

Introduction

Heterodinuclear complexes[1] and heterobimetallic clusters[2] have attracted much attention not only as organometallic models of active sites in heterogeneous bimetallic catalysts but also as potential precursors in homogeneous catalysis. In particular, interest has been focused on the heterodinuclear complexes containing organic groups,[3] since these complexes would offer fundamental information relevant to the behavior of organic species on the surface of heterogeneous bimetallic catalysts in processes such as naphtha-reforming[4] and Fischer–Tropsch[5] reactions.

We previously reported that the metathetical reactions of PtRCl(cod) (cod = 1,5-cyclooctadiene) with Na[WCp(CO)$_3$] provided (cod)RPt–WCp(CO)$_3$ (R = Me, Et, Ph, 2-MeC$_6$H$_4$).[6] An X-ray diffraction study on (cod)PhPt–WCp(CO)$_3$ showed that the complex had a cova-

[†] Department of Applied Chemistry, Osaka University.

[‡] Present address: Department of Chemistry, Faculty of Science, Kyoto University, Sakyo-ku, Kyoto 606, Japan

[⊗] Abstract published in *Advance ACS Abstracts*, September 1, 1994.

(1) (a) Bullock, R. M.; Casey, C. P. *Acc. Chem. Res.* **1987**, *20*, 167. (b) Stephan, D. W. *Coord. Chem. Rev.* **1989**, *95*, 41. (c) Ozawa, F.; Park, J. W.; Machenzie, P. B.; Schaefer, W. P.; Henling, L. M.; Grubbs, R. H. *J. Am. Chem. Soc.* **1989**, *111*, 1319. (d) Hosteler, M. J.; Bergman, R. G. *J. Am. Chem. Soc.* **1990**, *112*, 8621. (e) Ojima, I.; Okabe, K.; Kato, K.; Kwon, H. B.; Horváth, F. R. *J. Am. Chem. Soc.* **1988**, *110*, 150. (f) Gelmini, L.; Stephan, D. W. *Organometallics* **1988**, *7*, 849.

(2) (a) Shriver, D. F.; Kaesz, H.; Adams, R. D., Eds. *The Chemistry of Metal Cluster Complexes*; VCH Publishers: New York, 1990. (b) Gates, B. C.; Guczi, L.; Knözinger, H., Eds. *Metal Clusters in Catalysis*; Elsevier: Amsterdam, 1986. (c) Basset, J.-M.; Gates, B. C.; Candy, J. P.; Choplin, A.; Leconte, M.; Quignard, F.; Santini, C., Eds. *Surface Organometallics Chemistry: Molecular Approaches to Surface Catalysis*, Kluwer: Amsterdam, 1988. (d) Johnson, B. F. G., Ed. *Transition Metal Clusters*, Wiley: Chichester, 1980. (e) Süss-Fink, G.; Neumann, F. In *The Chemistry of the Metal-Carbon Bond*; Hartley, F. R., Ed.; Wiley: New York, 1989; Vol. 5, p 231. (f) Braunstein, P.; Rosé, J. In *Stereochemistry of Organometallic and Inorganic Compounds*; Bernal, I., Ed.; Elsevier: Amsterdam, 1988; Vol. 3, p 3. (g) Gladfelter, W. L.; Geoffroy, G. L. *Adv. Organomet. Chem.* **1980**, *18*, 207. (h) Roberts, D. A.; Geoffroy, G. L. In *Comprehensive Organometallic Chemistry*; Wilkinson, G.; Stone, F. G. A.; Abel, E. W., Eds.; Pergamon Press: Oxford, 1982; Vol. 6, p 763. (i) Vahrenkamp, H. *Adv. Organomet. Chem.* **1983**, *23*, 169. (j) Vargas, M. D.; Nicholls, J. N. *Adv. Inorg. Chem. Radiochem.* **1986**, *30*, 123. (k) Süss-Fink, G.; Meister, G. *Adv. Organomet. Chem.* **1993**, *35*, 41.

(3) For recent examples: (a) Baxter, S. M.; Ferguson, G. S.; Wolczanski, P. T. *J. Am. Chem. Soc.* **1988**, *110*, 4231. (b) Park, J. W.; Mackenzie, P. B.; Schaefer, W. P.; Grubbs, R. H. *J. Am. Chem. Soc.* **1986**, *108*, 6402. (b) Antwi-Nsiah, F.; Cowie, M. *Organometallics* **1992**, *11*, 3157.

(4) (a) Jinfelt, J. H. In *Catalysis—Science and Technology*, Anderson, J. R.; Boudard, M., Eds.; Springer-Verlag: Berlin, 1981; Vol. 1, p 257. (b) Biswas, J.; Bickle, G. M.; Gray, P. G.; Do, D. D.; Barbier, J. *Catal. Rev.-Sci. Eng.* **1988**, *30*, 161. (c) Shum, V. K.; Butt, J. B.; Sachtler, W. M. H. *J. Catal.* **1985**, *96*, 371. (d) Kim, C.; Somorjai, G. A. *Ibid.* **1992**, *134*, 179.

(5) (a) Falbe, J., Ed. *New Synthesis with Carbon Monoxide*, Springer-Verlag: Berlin, 1980. (b) Keim, W., Ed. *Catalysis in C1 Chemistry*; D. Reidel: Dordrecht, 1983. (c) Lee, G. v. d.; Ponec, V. *Catal. Rev.-Sci. Eng.* **1987**, *29*, 183.

(6) Komiya, S.; Endo, I. *Chem. Lett.* **1988**, 1709.

0276-7333/94/2313-4033$04.50/0

lent Pt–W bond (2.844 Å).[7] Notably, the methyl group on Pt migrated selectively to W on the thermolysis and this migration was greatly promoted by PPh_3, CO, and maleic anhydride. In the present study, we have synthesized and characterized a series of heterodinuclear Pt–W and –Mo complexes with various organic groups on Pt. Their reactivity in the organic group migration and the reaction mechanism have been studied.

Results and Discussion

Synthesis and Characterization of Heterodinuclear Complexes. Metathetical reactions of PtRCl(cod) with Na[M(CP)(CO)$_3$] (M = W, Mo; CP = Cp, C_5H_4Me, C_5H_4COOMe) in THF have afforded new heterodinuclear complexes (cod)RPt–M(CP)(CO)$_3$ with various organic groups (eq 1). In the cases that R = ortho-substituted aryls, *in situ* prepared nitrato complexes PtR(NO_3)(cod) were employed as precursors to allow the metathesis reactions to proceed more smoothly. The nitrato complexes were also used in the preparation of **2a**, **2b**, **3a**, and **3b** having Me or COOMe in CP. All the heterodinuclear complexes have been obtained as crystals by recrystallization from THF/hexane or CH_2Cl_2/hexane, and the crystals are moderately air-stable.

$$\text{PtRX(cod)} + \text{Na[M(CP)(CO)}_3\text{]} \rightarrow \text{(cod)RPt–M(CP)(CO)}_3 + \text{NaX} \quad (1)$$

1a–4c

R	X	M	CP	
Me	Cl	W	Cp	**1a**
Et	Cl	W	Cp	**1b**
Ph	Cl	W	Cp	**1c**
2-MeC_6H_4	NO_3	W	Cp	**1d**
4-MeC_6H_4	Cl	W	Cp	**1e**
2,6-$(Me)_2C_6H_3$	NO_3	W	Cp	**1f**
4-$MeOC_6H_4$	Cl	W	Cp	**1g**
C_6F_5	NO_3	W	Cp	**1h**
4-FC_6H_4	Cl	W	Cp	**1i**
4-ClC_6H_4	Cl	W	Cp	**1j**
Me	NO_3	W	C_5H_4Me	**2a**
Ph	NO_3	W	C_5H_4Me	**2b**
Me	NO_3	W	C_5H_4COOMe	**3a**
Ph	NO_3	W	C_5H_4COOMe	**3b**
Me	Cl	Mo	Cp	**4a**
Ph	Cl	Mo	Cp	**4b**
2-MeC_6H_4	Cl	Mo	Cp	**4c**

As is summarized in Experimental Section, elemental analyses gave satisfactory results for the new complexes except **1f**, **1g**, **1j**, and **3b**. Molar electric conductivity of **1a–4c** in THF is significantly small, suggesting that they are not ionic complexes but neutral ones. In UV-vis spectroscopy, **1a** in THF has a band at 285 nm which is not observed for the precursors PtMeCl(cod) and Na[WCp(CO)$_3$]. The band appears to be correlated with the presence of a Pt–W bond. Similar absorption bands are observed at 283–303 nm for the other heterodinuclear complexes.

In ^{1}H NMR spectroscopy of **1a–4c** (Table 1), COD ligands give two kinds of signals of olefinic protons having ^{195}Pt satellites. The olefinic protons *trans* to R give lower field signals with smaller J_{PtH} values than those *trans* to W (or Mo), implying stronger *trans* influence[8] of R than that of W or Mo in the square planar geometry at Pt. In the case of **1d** and **4c**, four olefinic protons of COD are not magnetically equivalent to give four sets of signals. This fact suggests that the aromatic rings of 2-MeC_6H_4 in **1d** and **4c** are fixed perpendicular to the coordination planes. For the complexes **1h–j** having F or Cl in R, signals of Cp and COD's olefinic protons shifted slightly to high field compared to the phenyl complex **1c**, indicating that they are weakly deshielded due to decrease in the electron density at the olefinic π bond through Pt.

IR spectra of the heterodinuclear complexes show strong ν_{CO} bands at *ca.* 1900 and 1800 cm^{-1}. The frequencies of **1a** (ν_{CO} (KBr) = 1894, 1795 cm^{-1}) resemble those of anionic Na[WCp(CO)$_3$] (1907, 1772 cm^{-1}) rather than neutral MeWCp(CO)$_3$ (2008, 1900br cm^{-1}). This implies that the back-bonding from W to the carbonyl ligands is strong in **1a**. Although **1a** has the formal oxidation states of Pt(I) and W(I), the real ones are likely to be close to Pt(II) and W(0), respectively.

Acidolysis of **1a** and **4a** with concentrated sulfuric acid liberated CH_4 in 97 and 91% yields, respectively, confirming the presence of a methyl group. Iodination of **1a** revealed that the reactivity of Pt–W bond is higher than that of Pt–Me; **1a** in C_6D_6 was treated with I_2 and after 30 min ^{1}H NMR showed the formation of PtMeI(cod) (54% yield) and WCp(CO)$_3$I (46%). The signals of PtMeI(cod) disappeared in 4 h, and those of WCp(CO)$_3$I (66%) and MeI (66%) were observed. The final Pt product could be PtI_2(cod), but the peaks of PtI_2(cod) were very small due to its low solubility in C_6D_6. These results can be interpreted as follows: the Pt–W bond is weak to be cleaved by I_2 to form PtMeI(cod) and WCp(CO)$_3$I, and the resulting PtMeI(cod) reacts further with I_2 to give PtI_2(cod) and MeI.

Molecular Structure of 4b. Complex **4b** has been subjected to single-crystal X-ray diffraction study. Crystal data are summarized in Table 2, and fractional atomic coordinates of non-H atoms are listed in Table 3. Selected bond distances and angles are listed in Table 4, and an ORTEP drawing is depicted in Figure 1. The crystal system and the molecular structure of **4b** are almost the same as those of the Pt–W analogue **1c** determined previously.[7] The Pt–Mo bond distance is 2.832(1) Å, which is in the typical range of Pt–Mo bonds (2.65–2.84 Å) reported for the cluster complexes such as $Pt_2Mo_2Cp_2(CO)_6L_2$ (L_2 = dpe and $2PEt_3$).[9] The geometries around Pt and Mo in **4b** are square planar and square pyramidal, respectively. These structural features are consistent with the electronic configurations of d^8 Pt(II) and d^6 Mo(0), as suggested by ^{1}H NMR and IR. For the bond of COD and Pt, the Pt–C(11) and Pt–C(12) bond lengths (2.372(13), 2.340(15) Å) *trans* to Ph are obviously longer than the Pt–C(7) and Pt–C(8) bond lengths (2.220(15), 2.196(15) Å) *trans* to Mo. This reflects stronger *trans* influence of Ph than that of MoCp(CO)$_3$.

(7) Miki, K.; Kasai, N.; Endo, I.; Komiya, S. *Bull. Chem. Soc. Jpn.* **1989**, *62*, 4033.

(8) (a) Yamamoto, A. *Organotransition Metal Chemistry—Fundamental Concepts and Applications*; Wiley: New York, 1986; p 179. (b) Collman, J. P.; Hegedus, L. S.; Norton, J. R.; Finke, R. G. *Principles and Applications of Organotransition Metal Chemistry*, University Science Books: Mill Valley, 1987; p 242. (c) Crabtree, R. H. *The Organometallic Chemistry of the Transition Metals*, Wiley: New York, 1988; p 6.

(9) (a) Braunstein, P.; Jud, J.-M. *Organometallics* **1983**, *2*, 180. (b) Bender, R.; Braunstein, P.; Jud, J.-M.; Dusausoy, Y. *Inorg. Chem.* **1984**, *23*, 4489.

Table 1. Selected ^{1}H NMR Data for the Heterodinuclear Complexes (cod)RPt–M(CP)(CO)$_3$[a]

complex				R			CP	=CH– (cod)	
R	M	CP		δ	J_{PtH}, Hz	J_{HH}, Hz	δ	δ	J_{PtH}, Hz
Me	W	Cp	**1a**	1.21 (s, 3H)	75.4		4.92 (s, 5H)	5.24 (br, 2H)	38
								4.42 (br, 2H)	59
Et	W	Cp	**1b**	1.58 (t, 3H)	86.3	7.6	4.97 (s, 5H)	5.50 (br, 2H)	33
				1.98 (q, 2H)	48.6	7.6		4.40 (br, 2H)	65
Ph	W	Cp	**1c**	7.35 (dd, 2H, *o*-)	51.3	7.8, 1.3	4.59 (s, 5H)	5.61 (br, 2H)	26
				6.95 (t, 2H, *m*-)		7.8, 7.8		4.59 (br, 2H)	63
				6.68 (t, 1H, *p*-)		7.8			
2-MeC$_6$H$_4$	W	Cp	**1d**	7.47 (dd, 1H, *o*-)	53.2	9, 2	4.58 (s, 5H)	5.67 (m, 1H)	
				6.90 (dt, 2H, *m*-)		9, 9, 2		5.51 (m, 1H)	
				6.69 (dt, 1H, *p*-)		9, 9, 2		4.47 (m, 1H)	64
				2.54 (s, 3H, *Me*)	6.4			4.18 (m, 1H)	60
4-MeC$_6$H$_4$	W	Cp	**1e**	7.28 (d, 2H, *o*-)	83.2	8.6	4.63 (s, 5H)	5.61 (br, 2H)	27
				6.89 (d, 2H, *m*-)		8.6		4.62 (br, 2H)	64
				2.17 (s, 3H, *Me*)					
2,6-(Me)$_2$C$_6$H$_4$	W	Cp	**1f**	6.92 (d, 1H, *m*-)		7.1	4.57 (s, 5H)	5.55 (br, 2H)	29
				6.86 (d, 1H, *m*-)		7.9		3.91 (br, 2H)	56
				6.73 (dd, 1H, *p*-)		7.9, 7.1			
				2.70 (s, 6H, *Me*)	8.0				
4-MeOC$_6$H$_4$	W	Cp	**1g**	7.22 (d, 2H, *o*-)	83.2	8.6	4.64 (s, 5H)	5.61 (br, 2H)	29
				6.76 (d, 2H, *m*-)		8.6		4.64 (br, 2H)	63
				3.36 (s, 3H, O*Me*)					
C$_6$F$_5$	W	Cp	**1h**				4.43 (s, 5H)	5.38 (br, 2H)	41
								4.37 (br, 2H)	54
4-FC$_6$H$_4$	W	Cp	**1i**	7.13 (dd, 2H, *o*-)[b]	83.2	8.9	4.55 (s, 5H)	5.56 (br, 2H)	24
				6.78 (t, 2H, *m*-)[c]		8.9		4.44 (br, 2H)	66
4-ClC$_6$H$_4$	W	Cp	**1j**	7.13 (d, 2H, *o*-)	83.2	7.4	4.54 (s, 5H)	5.55 (br, 2H)	37
				7.03 (d, 2H, *m*-)		7.4		4.42 (br, 2H)	70
Me	W	C$_5$H$_4$Me	**2a**	1.20 (s, 3H)	75.9		4.88 (s, 4H)	5.31 (br, 2H)	28
							1.95 (s, 3H)	4.42 (br, 2H)	60
Ph	W	C$_5$H$_4$Me	**2b**	7.37 (d, 2H, *o*-)	52.6		4.54 (m, 2H)	5.61 (br, 2H)	24
				7.01 (t, 2H, *m*-)			4.41 (m, 2H)	4.65 (br, 2H)	76
				6.70 (t, 1H, *p*-)			1.84 (s, 3H)		
Me	W	C$_5$H$_4$COOMe	**3a**	1.19 (s, 3H)	76.4		5.80 (t, 2H)	5.24 (br, 2H)	34
							4.78 (t, 2H)	4.41 (br, 2H)	65
							3.44 (s, 3H)		
Ph	W	C$_5$H$_4$COOMe	**3b**	7.29 (d, 2H, *o*-)	51.3		5.69 (t, 2H)	5.49 (br, 2H)	31
				6.95 (t, 2H, *m*-)			4.18 (t, 2H)	4.59 (br, 2H)	65
				6.66 (t, 1H, *p*-)			3.43 (s, 3H)		
Me	Mo	Cp	**4a**	1.14 (s, 3H)	75.0		4.95 (s, 5H)	5.2 (br, 2H)	32
								4.5 (br, 2H)	64
Ph	Mo	Cp	**4b**	7.36 (d, 2H, *o*-)	51.3	7.6	4.64 (s, 5H)	5.6 (br, 2H)	28
				6.99 (m, 2H, *m*-)				4.6 (br, 2H)	64
				6.69 (t, 1H, *p*-)					
2-MeC$_6$H$_4$	Mo	Cp	**4c**	7.50 (d, 1H, *o*-)	54.0	7.3	4.63 (s, 5H)	5.6 (m, 1H)	
				6.94 (m, 2H, *m*-)				5.5 (m, 1H)	
				6.72 (m, 1H, *p*-)				4.6 (m, 1H)	
				2.55 (s, 3H, Me)	6.1			4.5 (m, 1H)	

[a] In C_6D_6 at room temperature. [b] J_{FH} = 7.4 Hz. [c] J_{FH} = 8.9 Hz.

Among three carbonyl groups attached to Mo, two of them (C(21)–O(2) and C(22)–O(3)) are located as if attacking the Pt–Mo bond from the both sides. Although the Pt···C(21) and Pt···C(22) distances of 2.435(13) and 2.469(15) Å are much longer than those expected for the Pt–C bond as μ-CO ligands, the Mo–C(21) and Mo–C(22) bonds of 1.996(13) and 1.968(15) Å are lengthened and the Mo–C(21)–O(2) and Mo–C(22)–O(3) angles of 166.0(12)° and 169.7(13)° are slightly bent when compared to the other terminal CO; Mo–C(20) = 1.904(16) Å and Mo–C(20)–O(1) = 177.4(14)°. These facts imply that the two CO ligands have weak interaction with Pt.[10]

Organic Group Migration. Thermolysis. Treatment of (cod)RPt–M(CP)(CO)$_3$ in C_6D_6 at 70 °C for 2 h led to the migration of R from Pt to W (or Mo), *i.e.*, the reductive elimination of RM(CP)(CO)$_3$ (eq 2). The products and yields are listed in Table 5.

(10) ^{13}C{^{1}H} NMR was carried out for **1d**, but Pt satellites were not observed for ^{13}CO resonances for the semibridging carbonyls. See Experimental Section.

Table 2. Crystal Data for (cod)PhPt–MoCp(CO)$_3$ (4b)

formula	$C_{22}H_{22}O_3MoPt$
fw	625.43
cryst dimens, mm	0.10 × 0.50 × 0.70
F(000)	1192
cryst system	monoclinic
space group	$P2_1/n$
a, Å	14.291(5)
b, Å	12.738(3)
c, Å	11.988(4)
β, deg	112.01(3)
V, Å^3	2023.3(11)
Z	4
D_c, g cm^{-3}	2.053
μ, cm^{-1}	78.9
temp	room temp
radiation (wavelength, Å)	Mo Kα (0.71069)
monochromator	graphite
scan	θ–2θ scan
2θ max	54.0°
no. of collected reflns	4433
no. of unique reflns	3719 ($\|F_o\| > 3\,\sigma(\|F_o\|)$)
R^a	0.057
R_w^b	0.078

[a] $R = \Sigma||F_o| - |F_c||/\Sigma|F_o|$. [b] $R_w = [\Sigma\, w(|F_o| - |F_c|)^2/\Sigma\, w|F_o|^2]^{1/2}$.

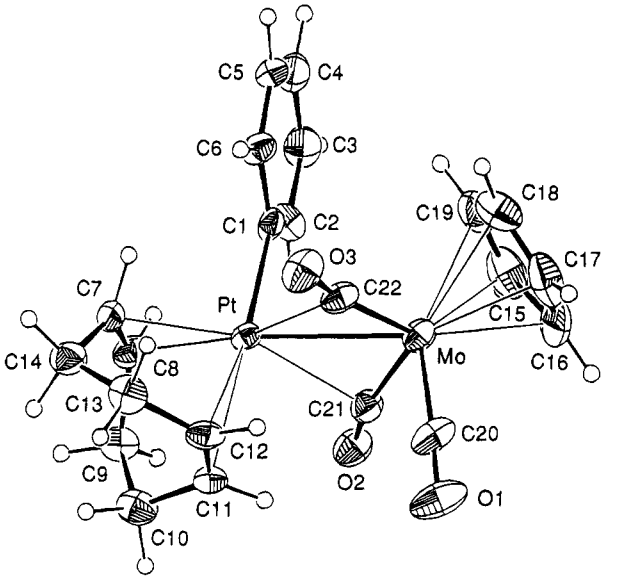

Figure 1. ORTEP drawing of (cod)PhPt−MoCp(CO)$_3$ (**4b**). Non-H atoms are represented by thermal ellipsoids at 30% probability levels, while H atoms are drawn by spheres with B = 1.0 Å^2.

Table 3. Fractional Atomic Coordinates and (Equivalent) Isotropic Thermal Parameters of Non-Hydrogen Atoms with Esd's for (cod)PhPt-MoCp(CO)$_3$ (4b)

atom	x	y	z	B_{eq} (Å^2)
Pt	0.39900(3)	0.27693(3)	0.27837(4)	2.9
Mo	0.54907(8)	0.36694(7)	0.20703(9)	3.7
C(1)	0.4559(8)	0.1372(8)	0.2458(12)	3.6
C(2)	0.5301(10)	0.0857(10)	0.3342(11)	4.0
C(3)	0.5664(11)	−0.0090(10)	0.3120(16)	5.4
C(4)	0.5190(11)	−0.0540(10)	0.1981(17)	5.6
C(5)	0.4406(11)	−0.0066(10)	0.1100(14)	4.9
C(6)	0.4069(10)	0.0885(9)	0.1337(12)	4.1
C(7)	0.2598(9)	0.2048(9)	0.2851(13)	3.9
C(8)	0.3341(11)	0.1968(9)	0.3949(12)	4.2
C(9)	0.3483(11)	0.2646(10)	0.5031(13)	4.6
C(10)	0.3215(11)	0.3818(12)	0.4721(12)	5.0
C(11)	0.3545(9)	0.4221(8)	0.3722(11)	3.7
C(12)	0.2959(11)	0.4245(8)	0.2553(12)	4.2
C(13)	0.1903(10)	0.3781(12)	0.1959(13)	4.9
C(14)	0.1717(10)	0.2756(10)	0.2501(14)	4.8
C(15)	0.7001(13)	0.2742(15)	0.2472(17)	6.7
C(16)	0.7089(15)	0.3851(22)	0.2089(24)	10.6
C(17)	0.6442(14)	0.3899(15)	0.0902(19)	7.2
C(18)	0.6021(15)	0.2933(15)	0.0582(16)	6.7
C(19)	0.6374(15)	0.2300(12)	0.1561(20)	6.8
C(20)	0.5271(11)	0.5135(10)	0.2170(11)	4.9
C(21)	0.5659(9)	0.3530(9)	0.3794(11)	3.9
C(22)	0.4078(10)	0.3561(9)	0.0946(11)	4.2
O(1)	0.5106(10)	0.6043(8)	0.2252(11)	7.2
O(2)	0.5960(7)	0.3480(8)	0.4827(8)	5.0
O(3)	0.3282(8)	0.3546(9)	0.0134(9)	5.7

This migration process is unusual, since there are few reports of the reductive elimination from *cis*-diorganoplatinum(II) complexes; one example is *cis*-Pt(4-MeC$_6$H$_4$)$_2$(PPh$_3$)$_2$ to give 4,4′-dimethylbiphenyl.[11] In the thermolysis of **1b**, EtWCp(CO)$_3$ formed is thermally unstable to decompose into C$_2$H$_4$ and C$_2$H$_6$. We were unable to fully characterize the Pt product in the thermolysis reactions (eq 2), but it seems to be some Pt(0) complex from the following experiments. The benzene solution of **1a** with excess PPh$_3$ was stirred for 4 h at room temperature, and after addition of excess MeI the solution was further stirred for 1 day. ^{1}H NMR spectrum of the resulting brown precipitate showed the formation of MeWCp(CO)$_3$ and PtMeI(PPh$_3$)$_2$ (25% yield from **1a**). We suppose that the Pt(0) complex formed in the thermolysis reacts with PPh$_3$ to give Pt(PPh$_3$)$_n$ (n = 3, 4), and that the oxidative addition of MeI yields PtMeI(PPh$_3$)$_2$.

(11) Braterman, P. S.; Cross, R. J.; Young, G. B. *J. Chem. Soc., Dalton Trans.* **1977**, 1892.

Table 4. Selected Bond Lengths and Angles for (cod)PhPt−MoCp(CO)$_3$ (4b)

Bond Lengths, Å			
Pt−Mo	2.8320(12)	Pt−C(1)	2.054(14)
Pt−C(7)	2.220(15)	Pt−C(8)	2.196(15)
Pt−C(11)	2.372(13)	Pt−C(12)	2.340(15)
Pt−C(21)	2.435(13)	Pt−C(22)	2.469(15)
Mo−C(15)	2.346(20)	Mo−C(16)	2.287(29)
Mo−C(17)	2.308(23)	Mo−C(18)	2.376(22)
Mo−C(19)	2.364(25)	Mo−C(20)	1.904(16)
Mo−C(21)	1.996(13)	Mo−C(22)	1.968(15)
C(20)−O(1)	1.19(3)	C(21)−O(2)	1.15(2)
C(22)−O(3)	1.19(2)		
Bond Angles, deg			
Mo−Pt−C(1)	84.0(4)	Mo−Pt−C(7)	165.7(4)
Mo−Pt−C(8)	158.2(4)	Mo−Pt−C(11)	101.3(4)
Mo−Pt−C(12)	98.9(4)	Mo−Pt−C(21)	43.7(4)
Mo−Pt−C(22)	42.9(4)	C(1)−Pt−C(7)	94.1(6)
C(1)−Pt−C(8)	90.6(6)	C(1)−Pt−C(11)	164.0(5)
C(1)−Pt−C(12)	161.8(6)	C(1)−Pt−C(21)	93.2(5)
C(1)−Pt−C(22)	91.6(6)	C(21)−Pt−C(22)	85.0(5)
Pt−Mo−C(20)	102.5(5)	Pt−Mo−C(21)	57.5(4)
Pt−Mo−C(22)	58.7(5)	C(20)−Mo−C(21)	88.9(6)
C(20)−Mo−C(22)	87.8(7)	C(21)−Mo−C(22)	113.4(6)
Mo−C(20)−O(1)	177.4(14)	Mo−C(21)−O(2)	166.0(12)
Mo−C(22)−O(3)	169.7(13)		

Table 5. Thermolysis of the Heterodinuclear Complexes[a]

complex	product[b]	yield, %[b]
(cod)MePt−WCp(CO)$_3$ (**1a**)	MeWCp(CO)$_3$	73
(cod)EtPt−WCp(CO)$_3$ (**1b**)[c]	EtWCp(CO)$_3$	9[d]
(cod)PhPt−WCp(CO)$_3$ (**1c**)	PhWCp(CO)$_3$	51
(cod)(2-MeC$_6$H$_4$)Pt−WCp(CO)$_3$ (**1d**)	(2-MeC$_6$H$_4$)WCp(CO)$_3$	25
(cod)(4-MeC$_6$H$_4$)Pt−WCp(CO)$_3$ (**1e**)	(4-MeC$_6$H$_4$)WCp(CO)$_3$	44
(cod)(2,6-(Me)$_2$C$_6$H$_3$)Pt−WCp(CO)$_3$ (**1f**)	(2,6-(Me)$_2$C$_6$H$_3$)WCp(CO)$_3$	29
(cod)(C$_6$F$_5$)Pt−WCp(CO)$_3$ (**1h**)	(C$_6$F$_5$)WCp(CO)$_3$	41
(cod)(4-FC$_6$H$_4$)Pt−WCp(CO)$_3$ (**1i**)	(4-FC$_6$H$_4$)WCp(CO)$_3$	53
(cod)(4-ClC$_6$H$_4$)Pt−WCp(CO)$_3$ (**1j**)	(4-ClC$_6$H$_4$)WCp(CO)$_3$	43
(cod)MePt−W(C$_5$H$_4$Me)(CO)$_3$ (**2a**)	MeW(C$_5$H$_4$Me)(CO)$_3$	50
(cod)PhPt−W(C$_5$H$_4$Me)(CO)$_3$ (**2b**)	PhW(C$_5$H$_4$Me)(CO)$_3$	59
(cod)MePt−W(C$_5$H$_4$COOMe)(CO)$_3$ (**3a**)	MeW(C$_5$H$_4$COOMe)(CO)$_3$	35
(cod)PhPt−W(C$_5$H$_4$COOMe)(CO)$_3$ (**3b**)	PhW(C$_5$H$_4$COOMe)(CO)$_3$	54
(cod)MePt−MoCp(CO)$_3$ (**4a**)	MeMoCp(CO)$_3$	45

[a] Solvent, C$_6$D$_6$; temperature, 70 °C; reaction time, 2 h. [b] Determined by ^{1}H NMR. [c] At 50 °C for 2 h. [d] Other products and yields: C$_2$H$_4$, 63%; C$_2$H$_6$, 8%.

$$\underset{\textbf{1a–4c}}{\text{(cod)RPt–M(CP)(CO)}_3} \xrightarrow[\text{C}_6\text{D}_6,\ 2\text{ h}]{\Delta\ (70\ ^\circ\text{C})} \text{RM(CP)(CO)}_3 \qquad (2)$$

M = W, Mo
CP = Cp, C_5H_4Me, C_5H_4COOMe

A crossover experiment was performed to examine the migration is *intra*- or *inter*molecular reaction. A mixture of (cod)(2-MeC$_6$H$_4$)Pt−WCp(CO)$_3$ (**1d**) and (cod)PhPt−W(C$_5$H$_4$Me)(CO)$_3$ (**2b**) dissolved in C$_6$D$_6$ was heated at 70 °C, and the reaction was followed by ^{1}H NMR. The products were (2-MeC$_6$H$_4$)WCp(CO)$_3$ and PhW(C$_5$H$_4$Me)(CO)$_3$, and their respective yields based on **1d** and **2b** were as follows: 15 and 30% after 15 min, 20 and 41% after 45 min, and 28 and 43% after 120 min. Neighter PhWCp(CO)$_3$ nor (2-MeC$_6$H$_4$)W(C$_5$H$_4$Me)(CO)$_3$ was not observed in ^{1}H NMR during the reaction. These

Table 6. Effect of Additives on the Methyl Migration for 1a To Form $MeWCp(CO)_3$[a]

additive	M	yield of $MeWCp(CO)_3$, %[b]
none	–	0
CO	(1 atm)	75
$P(OPh)_3$	1.1	69
PPh_3	2.4	58
$PMePh_2$	2.8	<1
PMe_2Ph	1.5	trace
PMe_3	1.1	trace
PCy_3	2.9	7
maleic anhydride	17.6	37
acrylonitrile	15.4	13
methacrylonitrile	10.0	trace
methyl acrylate	16.4	trace
trans-stilbene	14.3	trace
vinyl acetate	16.7	trace

[a] Solvent, C_6D_6; temperature, rt; reaction time, 2 h; [**1a**] = 0.038 M. [b] Determined by ^1H NMR.

results support that the organic group migration in the thermolysis is an *intra*molecular reaction.

Acceleration of Organic Group Migration by Additives. As is shown in Table 6, CO (1 atm) readily reacted with **1a** in C_6D_6 at room temperature to afford $MeWCp(CO)_3$. Similarly, addition of CO to the C_6D_6 solution of **1b**, **1c**, and **4a** gave $EtWCp(CO)_3$, $PhWCp(CO)_3$, and $MeMoCp(CO)_3$, respectively. Presumably, the coordination of a π-acidic CO ligand to Pt facilitates the reductive elimination.[12] $Pt(CO)_2(PPh_3)_2$ and $Pt(CO)(PPh_3)_3$[13] were produced when excess PPh_3 was added to the reaction mixture of **1a** and CO. These Pt carbonyl phosphine complexes may be formed via Pt(0) intermediates such as "$\{Pt(CO)_2\}_n$".

The acceleration of the reductive elimination was also observed when adding PPh_3 and $P(OPh)_3$. It is likely that PPh_3 and $P(OPh)_3$ coordinate to Pt to accelerate the reductive elimination, since the associative acceleration by PR_3 is well known for $PtAr_2L_2$,[11] NiMeAr(dmpe),[14] and Ni(aryl)(η^3-allyl)L.[15] In contrast, more basic phosphines such as $PMePh_2$, PMe_2Ph, and PMe_3 to **1a** did not afford $MeWCp(CO)_3$ but gave new ionic complexes $[PtMe(PR_3)_3]^+[WCp(CO)_3]^-$ (eq 3 for PMe_3). In eq 3, the COD ligand in **1a** is expected to be displaced by PMe_3 to form $[(Me_3P)_2MePt–WCp(CO)_3]$ due to the smaller cone angle and larger basicity of PMe_3. This type of Pt–W phosphine complex would be fairly stable; in fact, $(Ph_3P)_2MePt–WCp(CO)_3$[16] and (dpe)MePt–$WCp(CO)_3$[17] are isolated. Coordination of another PMe_3 molecule to Pt and the successive ionization can lead to the formation of **5**. Such ionization reactions are frequently observed for d^8 organometallic complexes.[18] On the other hand, the ionization was prevented in the reaction of **1a** with basic but bulkier PCy_3, and in this case $MeWCp(CO)_3$ was formed in a low yield (7%).

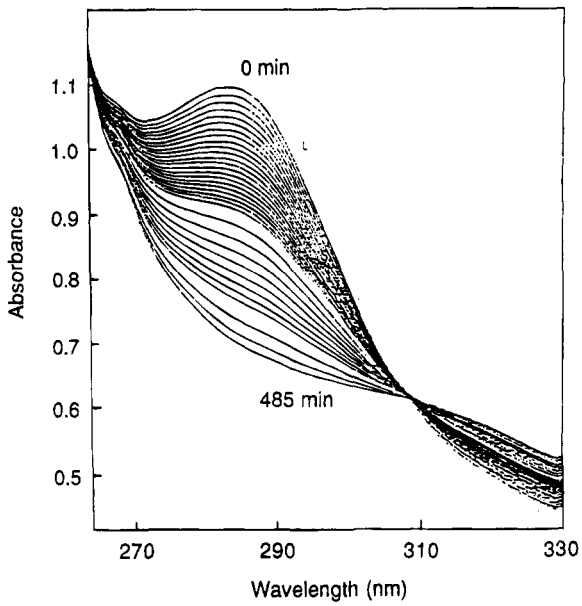

Figure 2. UV-vis spectral change of **1a** in the presence AN. Solvent, THF; temperature, 38 °C; [**1a**] = 2.1×10^{-5} M; [AN] = 0.10 M.

$$(cod)MePt–WCp(CO)_3 \xrightarrow[\text{benzene, rt}]{+ 2PMe_3,\ - COD} [(Me_3P)_2MePt–WCp(CO)_3] \xrightarrow{+ PMe_3} [PtMe(PMe_3)_3]^+[WCp(CO)_3]^- \quad (3)$$

1a **5**

As summarized in Table 6, olefins with electron-withdrawing groups such as maleic anhydride and acrylonitrile (AN) accelerate the methyl migration for **1a** (eq 4). Characterization of the Pt product has been unsuccessful, but some Pt(0) complex is plausible. Indeed, the reaction of An with (dpe)MePt–$FeCp(CO)_2$ produced (dpe)Pt(AN) and $MeFeCp(CO)_2$, and the former complex was isolated.[17] Only a trace amount of $MeWCp(CO)_3$ was obtained when using olefins with less electron-withdrawing groups such as methacrylonitrile, methyl acrylate, *trans*-stilbene, and vinyl acetate. AN also accelerates the phenyl migration for **1c**; the yield of $PhWCp(CO)_3$ is 16% under the same conditions of Table 6. However, maleic anhydride having more electron-withdrawing character did not cause the phenyl migration. Probably, the steric bulkiness of the disubstituted olefin discourages its coordination to Pt.

$$(cod)MePt–WCp(CO)_3 + AN \rightarrow MeWCp(CO)_3 + \text{"Pt(0)"} + COD \quad (4)$$

1a

Kinetic Study of the Organic Group Migration. As mentioned in the UV-vis spectroscopy of **1a**, the electronic absorption at 285 nm appears to be correlated with the presence of a Pt–W bond. Figure 2 demonstrates the UV-vis spectral changes of the reaction of **1a** with AN, in which an isosbestic point is observed at 307 nm to indicate the absence of stable intermediates. The rate of formation of $MeWCp(CO)_3$ is obtained by monitoring the decrease of [**1a**], and the first order plot of the reaction yields a straight line (Figure 3). Similar

(12) (a) Reference 8a, p 244. (b) Reference 8b, p 326.
(13) (a) Chini, J.; Chini, P. *J. Chem. Soc. (A)* **1970**, 1538. (b) Chini, P.; Longoni, G. *Ibid.* **1970**, 1542.
(14) (a) Komiya, S.; Abe, Y.; Yamamoto, T.; Yamamoto, A. *Organometallics* **1983**, *2*, 1466. (b) Tatsumi, K.; Nakamura, A.; Komiya, S.; Yamamoto, A.; Yamamoto, T. *J. Am. Chem. Soc.* **1984**, *106*, 8181.
(15) (a) Kurosawa, H.; Ohnishi, H.; Emoto, M.; Kawasaki, Y.; Murai, S. *J. Am. Chem. Soc.* **1988**, *110*, 6272. (b) Kurosawa, H.; Ohnishi, H.; Emoto, M.; Chatani, N.; Kawasaki, Y.; Murai, S.; Ikeda, I. *Organometallics* **1990**, *9*, 3038.
(16) Ferrer, M.; Rossell, O.; Seco, M.; Braunstein, P. *J. Chem. Soc., Dalton Trans.* **1989**, 379.
(17) Fukuoka, A.; Sadashima, T.; Sugiura, T.; Wu, X.; Mizuho, Y.; Komiya, S. *J. Organomet. Chem.* **1994**, *473*, 139.
(18) (a) Clark, H. C.; Ruddick, J. D. *Inorg. Chem.* **1970**, *9*, 1226. (b) Hooton, K. A. *J. Chem. Soc. A* **1970**, 1896. (c) Komiya, S.; Kochi, J. K. *J. Am. Chem. Soc.* **1976**, *98*, 7599.

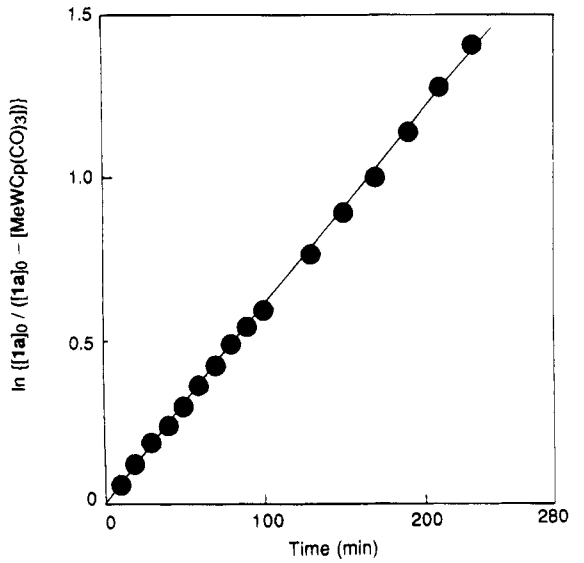

Figure 3. First-order plot of the reaction of **1a** with AN. Conditions: see Figure 2.

Table 7. Pseudo-First-Order Rate Constants for the Methyl Migration for 1a and 4a in the Presence of Olefins[a]

complex	olefin[b]	[olefin] M	$10^4 k_{obsd}$[c] s^{-1}
1a	AN	0.10	1.12
1a	AN	0.29	2.18
1a	AN	0.37	2.51
1a	AN	0.49	3.80
1a	AN	0.68	5.28
1a	AN	1.00	6.20
1a	MA	0.10	0.71
1a	MA	0.29	1.23
1a	MA	0.49	1.40
1a	MA	1.00	2.82
1a	VAc	0.10	0.66
1a	VAc	0.29	0.64
1a	VAc	0.49	0.72
1a	VAc	1.00	0.83
4a	AN	0.11	0.87
4a	AN	0.21	1.42
4a	AN	0.40	2.45
4a	AN	0.50	2.79
4a	AN	0.79	3.88
4a	AN	0.87	4.33
4a	MA	0.15	0.69
4a	MA	0.55	1.53
4a	MA	0.87	1.57
4a	MA	0.91	2.17
4a	VAc	0.16	0.52
4a	VAc	0.43	0.51
4a	VAc	0.89	0.58

[a] Solvent, THF; temperature, 38 °C for **1a** and 40 °C for **4a**; [**1a**] = (0.29−3.8) × 10^{-5} M, [**4a**] = (3.0−4.9) × 10^{-7} M. [b] AN = acrylonitrile, MA = methacrylonitrile, VAc = vinyl acetate. [c] Errors are ±0.07 × 10^{-4} s^{-1}.

first order plots have been obtained for the reactions of **1a** (or **4a**) with methacrylonitrile and vinyl acetate, and pseudo-first order rate constants (k_{obsd}) are estimated (Table 7).

A plot of k_{obsd} versus [olefin] yields straight lines and it can be written as

$$k_{obsd} = A + B[\text{olefin}] \qquad (5)$$

where A and B are constants (Figure 4).[19] The constant A corresponds to the thermolysis of **1a** (or **4a**). The values of B for three olefins are decreased by the following order: acrylonitrile > methacrylonitrile > vinyl acetate. The dependence of k_{obsd} on the concentration and nature of olefins indicates that an associative pathway through a π complex is involved in the reaction mechanism. This type of dependence of k_{obsd} was previously observed for the reductive elimination of R−R from NiR_2(bipy) (R = Me, Et; bipy = 2,2′-bipyridine) and the following mechanism was proposed; AN coordinates to Ni to form a π complex and the reductive elimination of R−R is promoted by a decrease of the electron density on Ni due to the back-bonding from Ni to AN.[20]

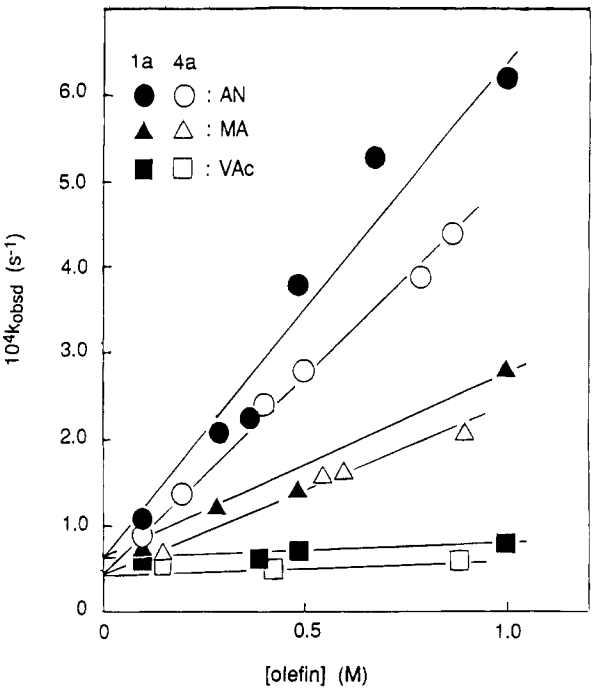

Figure 4. Plot of k_{obsd} vs [olefin] for the methyl migration for **1a** and **4a**: Solvent, THF; temperature, 38 °C for **1a** and 40 °C for **4a**; [**1a**] = (1.0−4.0) × 10^{-5} M; [**4a**] = (3.0−5.0) × 10^{-7} M.

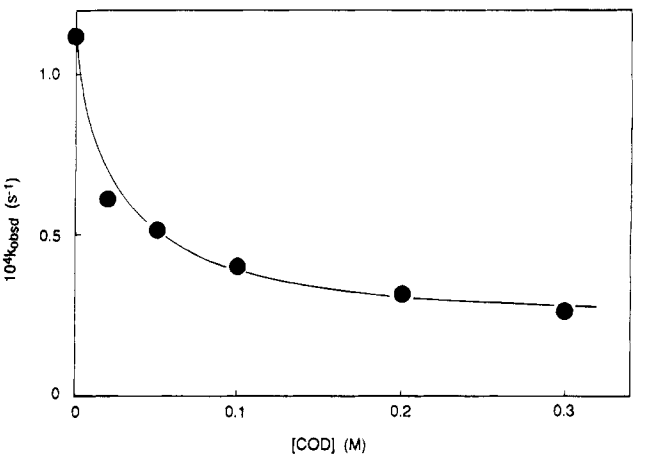

Figure 5. Plot of k_{obsd} vs [COD] for the methyl migration for **1a** in the presence of AN. Solvent, THF; temperature, 40 °C; [AN] = 0.10 M; [**1a**] = (1.9−4.6) × 10^{-7} M.

(19) The organic group migration for **1a**−**4c** was gradually accelerated in the absence of olefin and was not first order in the concentration of the complexes. This acceleration is presumably due to Pt(0) species formed during the reaction. Thus k_{obsd} values were estimated by an initial rate study at ca. 10% conversion of the complexes: 0.46 × 10^{-4} s^{-1} (at 38 °C) for **1a** and 0.36 × 10^{-4} s^{-1} (40 °C) for **4a**, respectively. These values are roughly the same as those obtained by extrapolating the k_{obsd} in the presence of olefins in Figure 4 (*i.e.*, intercept A). Accordingly, the values of the intercept A are used as k_{obsd} in the absence of olefin in the kinetic study below.

Scheme 1. Proposed Mechanism of Methyl Migration for (cod)MePt–WCp(CO)$_3$ (1a)

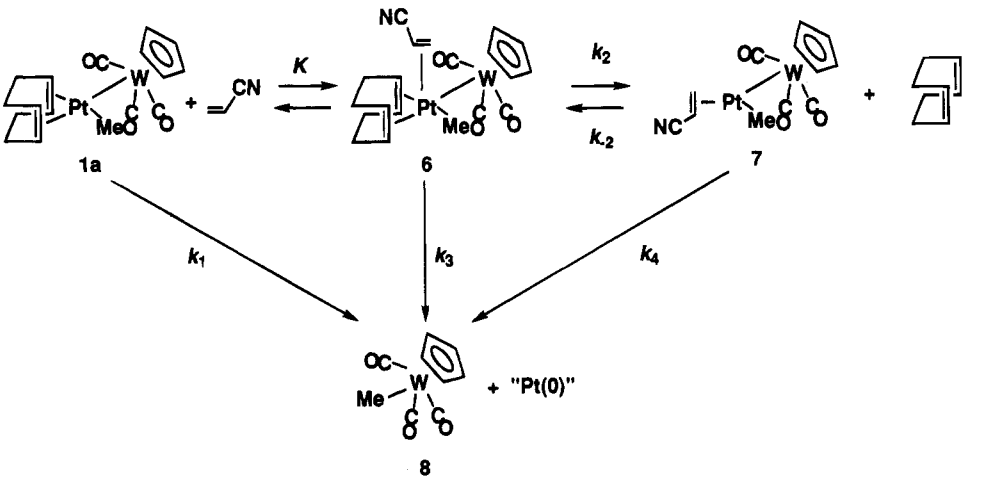

In contrast to the promotion effect of AN, addition of COD retards the methyl migration for **1a** in the presence of excess AN (Figure 5). This suggests that dissociation of COD is involved in the mechanism of the methyl migration.

In light of these considerations, we propose the mechanism for the organic group migration reactions (Scheme 1 for **1a**). Here we adopt the following assumptions: (1) a fast equilibrium exists between complex **1a** and a five-coordinated intermediate (**6**), (2) COD is dissociated from **6** to form a three-coordinated intermediate (**7**) and this step is rate-determining, (3) **7** is in steady-state, (4) MeWCp(CO)$_3$ (**8**) is produced from **1a**, **6**, and **7**. According to Scheme 1, the rate of formation of **8** can be written as

$$\begin{aligned} d[\mathbf{8}]/dt = &\{k_1k_4 + k_1k_{-2}[\mathrm{COD}] + \\ &k_4(k_2 + k_3)K[\mathrm{AN}] + \\ &k_{-2}k_3K[\mathrm{COD}][\mathrm{AN}]\}/ \\ &\{(k_4 + k_{-2}[\mathrm{COD}]) \times \\ &(1 + (1 + k_2)K[\mathrm{AN}])\} \times ([\mathrm{Pt}]_0 - [\mathbf{8}]) \\ = &\, k_{\mathrm{obsd}}([\mathrm{Pt}]_0 - [\mathbf{8}]) \end{aligned} \quad (6)$$

where $[\mathrm{Pt}]_0$ is the total concentration of platinum complexes and

$$\begin{aligned} k_{\mathrm{obsd}} = &\{k_1k_4 + k_1k_{-2}[\mathrm{COD}] + k_4(k_2 + k_3)K[\mathrm{AN}] + \\ &k_{-2}k_3K[\mathrm{COD}][\mathrm{AN}]\}/\{(k_4 + \\ &k_{-2}[\mathrm{COD}])(1 + (1 + k_2)K[\mathrm{AN}])\} \end{aligned} \quad (7)$$

With increasing [COD], k_{obsd} approaches a constant $(k_1 + k_3K[\mathrm{AN}])/\{1 + (1 + k_2)K[\mathrm{AN}]\}$, thus being in accordance with Figure 5. When [COD] = 0 in eq 7, k_{obsd} reduces

$$k_{\mathrm{obsd}} = \{k_1 + (k_2 + k_3)K[\mathrm{AN}]\}/\{1 + (1 + k_2)K[\mathrm{AN}]\} \quad (8)$$

Here it is possible to assume that $1 \gg (1 + k_2)K[\mathrm{AN}]$, since no other complexes than **1a** were observed in ^{1}H NMR or UV-vis during the reaction. Thus, k_{obsd} reduces

$$k_{\mathrm{obsd}} = k_1 + (k_2 + k_3)K[\mathrm{AN}] \quad (9)$$

Equation 9 is consistent with eq 5 derived from the experimental data. In eq 9, the k_1 term is the rate constant for the thermolysis and the $(k_2 + k_3)K[\mathrm{AN}]$ term is for the pathway involving AN. In order to clarify the influence of the nature of olefin on the latter term, $\log (k_2 + k_3)K$ versus Alfrey-Price's *e*-value of olefins has been plotted in Figure 6, where the *e*-value indicates electron-deficiency of substituted olefins.[21] Figure 6 clearly shows that the electron-deficient olefins enhance the methyl migration, as described for $NiR_2(bipy)$.[20]

Solvent Effect on the Methyl Migration. Reactions of complex **1a** and **4a** with added AN were carried out in various solvents, and k_{obsd} values were obtained. As seen in Figure 7 for **4a**, plotting k_{obsd} versus [AN] yields straight lines. It is found that the k_{obsd} values are independent of the nature of solvents at [AN] = 0 (*i.e.*, in the thermolysis). However, the k_{obsd} values in the presence of AN are greater in more polar solvents: acetonitrile > diisopropyl ether ≈ THF > dioxane ≈ toluene ≈ benzene. According to eq 9, the $(k_2 + k_3)K$ values are obtained from the slopes of the straight lines in Figure 7. To elucidate the transition state of the pathway involving AN, $\log(k_2 + k_3)K$ versus $(\epsilon - 1)/(2\epsilon + 1)$ (ϵ = dielectric constant of the solvent)[22] is plotted according to the Kirkwood's formula,[23] yielding a straight line with a positive slope (Figure 8). This may indicate extensive polarization and solvation at the transition state, where Pt and AN may be polarized by strong back-bonding from Pt to AN (Scheme 2). On the other hand, the transition state in the thermolysis is not influenced by the nature of solvents, since the plots of $\log k_1$ versus $(\epsilon - 1)/(2\epsilon + 1)$ yield a straight line with a slope of zero (Figure 9). Therefore, we suggest that a nonpolar three-center transition state is formed by Pt, W, and the Me carbon in the thermolysis. A similar solvent effect has been observed for complex **1a**.

Effect of Substituents in Cyclopentadienyl Ligand. The CP ligand in (cod)RPt–W(CP)(CO)$_3$ also

(20) Yamamoto, T.; Yamamoto, A.; Ikeda, S. *J. Am. Chem. Soc.* **1971**, *93*, 3350.

(21) (a) *Polymer Handbook*, 2nd ed.; Brandrup, J.; Immergut, E. H., Eds.; Wiley: New York, 1975. (b) Fujikura, J.; Tsuruta, T. *J. Polym. Sci.* **1959**, *36*, 257.

(22) ϵ of the solvent used: acetonitrile (37.5), diisopropyl ether (3.88), THF (7.58), dioxane (2.209), toluene (2.568), benzene (2.275). *Lange's Handbook of Chemistry*, 13th ed.; Dean, J. A., Ed.; McGraw-Hill: New York, 1985.

(23) Frost, A.; Pearson, R. G. *Kinetics and Mechanism*, 2nd ed.; Wiley: New York, 1961; p 140.

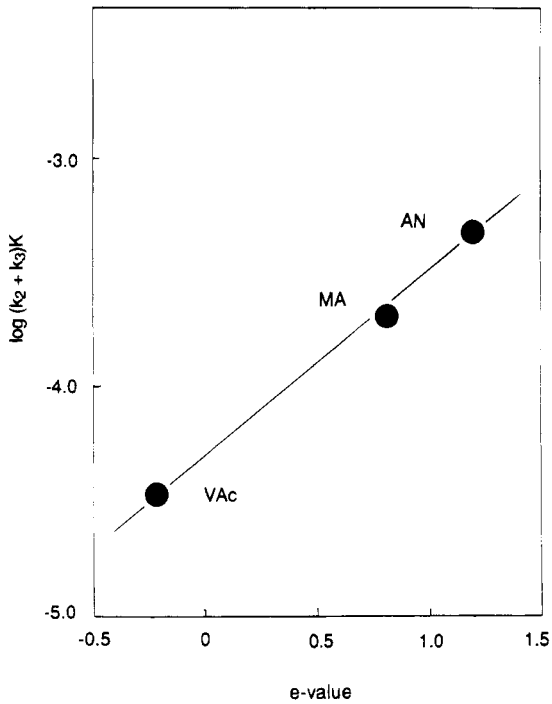

Figure 6. Plot of $\log(k_2 + k_3)K$ vs e-values of olefins. AN = acrylonitrile, MA = methacrylonitrile, VAc = vinyl acetate.

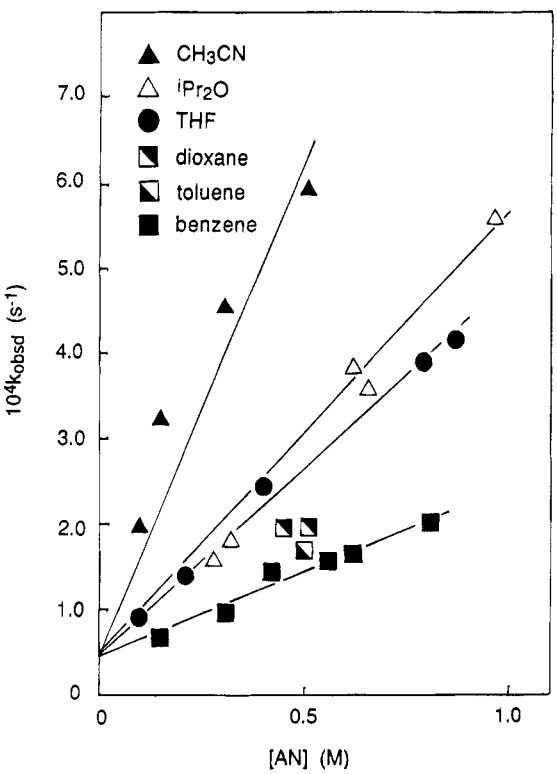

Figure 7. Solvent effect on k_{obsd} of the methyl migration for **4a** in the presence of AN. Temperature, 40 °C; [**4a**] = (2.6–7.3) × 10^{-7} M.

has influence on the organic group migration in the presence of excess AN. The k_{obsd} values are increased linearly with increasing in the concentration of AN (Figure 10), and the $(k_2 + k_3)K$ in k_{obsd} is estimated according to eq 9. The Me and Ph migrations are accelerated by Me in CP, whereas COOMe retards the migration. Perhaps, the Me group increases the electron density at Pt by way of W to facilitate the coordination of AN, which enhances the pathway from **6** to **8**.[24]

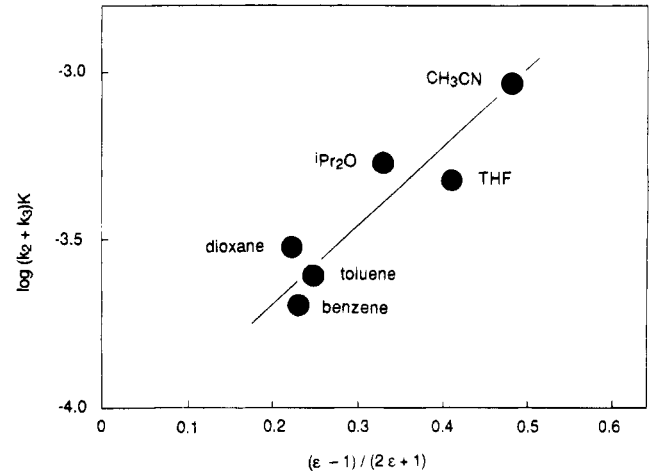

Figure 8. Plot of $\log(k_2 + k_3)K$ vs $(\epsilon - 1)/(2\epsilon + 1)$.

Scheme 2. Transition State of Methyl Migration for (cod)MePt–WCp(CO)$_3$ (1a)

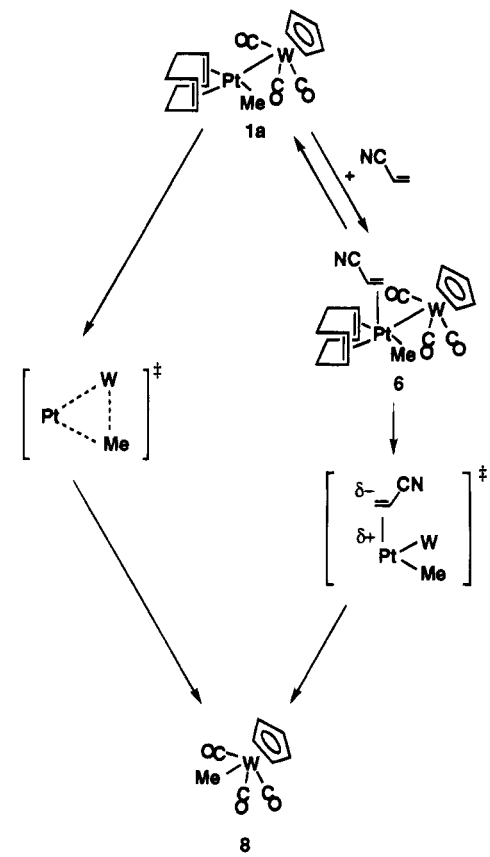

Effect of Organic Groups. Kinetic study of the organic group migration for complexes **1c–j** with various aryl groups has been similarly performed. The k_{obsd} value for the phenyl complex **1c** is larger than that for the methyl complex **1a** (Figure 10), showing that the Ph migration is more pronounced by AN than the Me migration. Similar higher reactivity of Ph than that of Me in reductive elimination was reported for *cis*-$AuMe_2$-

(24) Another explanation for the effect of CP is possible. If the transition state for the reductive elimination of RW(CP)(CO)$_3$ has some W(II) character, this can be stabilized by the better donor CP's.

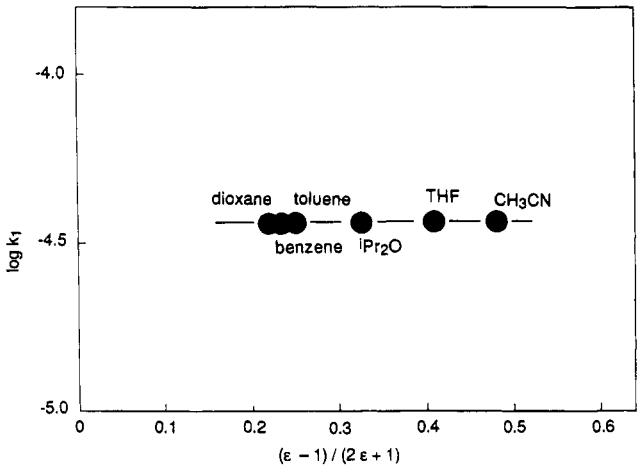

Figure 9. Plot of log k_1 vs $(\epsilon - 1)/(2\epsilon + 1)$.

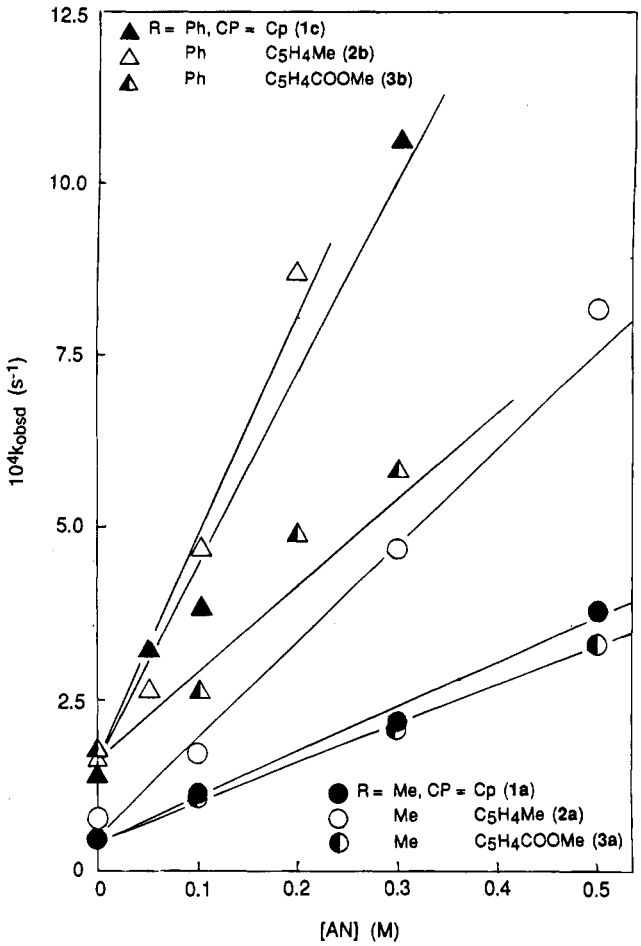

Figure 10. Plot of k_{obsd} vs [AN] for (cod)RPt–W(CP)(CO)$_3$. Solvent, THF; temperature, 40 °C; [complex] = (1–3) × 10^{-7} M.

PhL.[18c,25,26] In addition, it is suggested by using the extended Hückel method that activation energies of the formation of ethane (R = Me) and biphenyl (R = Ph) from *cis*-NiR_2H_2 are 1.4 and 0.7 eV, respectively,[27] and the smaller activation energy of Ph is ascribed to the interaction of pπ orbitals at α-positions in the two Ph's.[28,11] Accordingly, the higher reactivity of Ph over

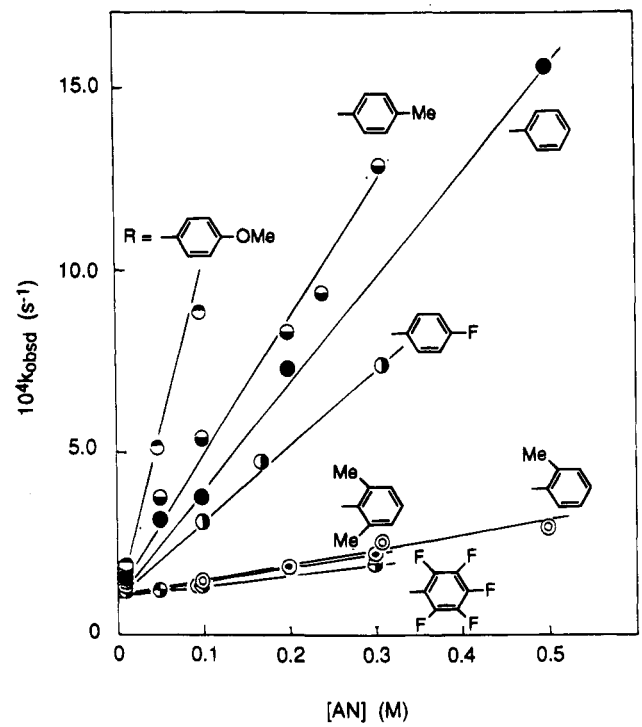

Figure 11. Plot of k_{obsd} vs [AN] for aryl complexes (cod)-RPt–WCp(CO)$_3$ (**1c–i**). Solvent, THF; temperature, 40 °C; [complex] = (0.7–8.8) × 10^{-7} M.

Me for (cod)RPt–WCp(CO)$_3$ may result from some interaction between a pπ-orbital of α-carbon in Ph and an empty d orbital of W.

The k_{obsd} values for the thermolysis are almost the same for **1c–j**,[29] but in the presence of excess AN k_{obsd} is increased linearly with increasing the concentration of AN (Figure 11). The $(k_2 + k_3)K$ values were estimated from the slopes, and a plot of $\log(k_2 + k_3)K$ versus the Hammett σ-values of the substituents at *para*-position of aryl groups gives a straight line with a slope of −0.3 (Figure 12). This indicates that the rate enhancement by AN is smaller for the complexes having more electron-withdrawing groups on the aryl groups. These groups prevent AN from coordinating to Pt, and thus the migration is not promoted in spite of the presence of excess AN. In addition, the rate enhancement by AN is small for the complexes having *ortho*-substituted aryls in Figure 11, which may result from steric hindrance of Me in the coordination of AN to Pt. From these considerations, we deduce that the contribution of K is greater to the $(k_2 + k_3)K$ term in eq 9 than that of $(k_2 + k_3)$.[30]

Conclusion

In the present study, we have synthesized the new Pt–W (or Mo) heterodinuclear complexes with alkyl and aryl ligands, and the complexes have been characterized by elemental analysis, NMR, IR, and chemical reactions. The molecular structure of (cod)PhPt–MoCp(CO)$_3$ is established by X-ray crystallography. The Pt–W and –Mo complexes undergo the alkyl or aryl group migration from Pt to W (or Mo) on thermolysis, and the

(25) Komiya, S.; Shibue, A. *Organometallics* **1985**, *4*, 684.
(26) Komiya, S.; Albright, T. A.; Hoffman, R.; Kochi, J. K. *J. Am. Chem. Soc.* **1976**, *98*, 7255.
(27) Tatsumi, K. Private communication.
(28) Low, J. J.; Goddard, A., III. *J. Am. Chem. Soc.* **1986**, *108*, 6115.
(29) As described in ref 19, in the thermolysis of complexes **1d–j** the rates were not first order in the concentration of the complexes. Thus, the k_{obsd} values for the thermolysis were obtained by extrapolating the k_{obsd} in the presence of AN.
(30) As a reviewer has commented, it is likely that k_3 is small, since electron-withdrawing groups on an aryl ring are known to increase the aryl-metal bond strength.

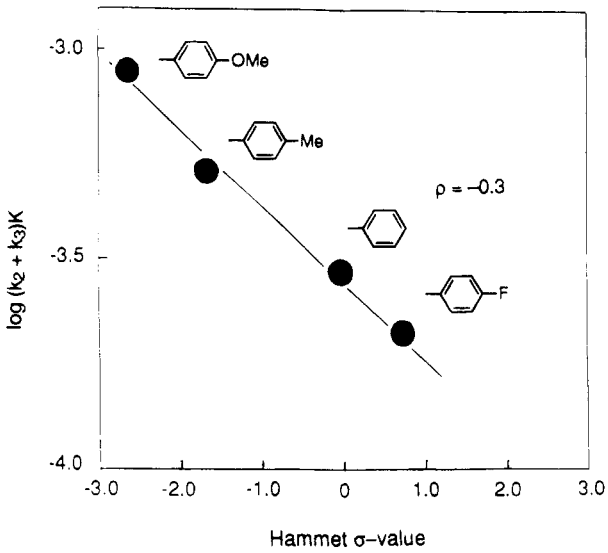

Figure 12. Plot of $\log(k_2 + k_3)K$ vs Hammett σ-value of the substituents at *para*-position of the aryl groups.

migration is accelerated by less basic tertiary phosphines, CO, and electron-deficient olefins. This acceleration can be explained by coordination of the additives to Pt to promote the reductive elimination of $RMCp(CO)_3$. Electron-donating groups in CP ligands on W (or Mo) and in aryl ligands on Pt increase the electron density at Pt to facilitate the coordination of AN, thus resulting in the rate enhancement of the organic group migration. Accordingly, it is suggested that the organic group migration for the heterodinuclear Pt−W (or −Mo) complexes is accelerated by the similar effects to those promoting the reductive elimination of R_2 from *cis*-PtR_2L_2.

Here we have shown the organic group migration on different two metals. The heterometallic migration of organic groups is important since the organic groups are considered as models of hydrocarbon species on heterogeneous bimetallic catalysts for naphtha-reforming the Fischer−Tropsch reactions. It is conceivable that the hydrocarbon species such as alkyl groups can be mobile on heterometallic site of the catalysts as spillover hydrocarbons.

Experimental Section

All manipulations were carried out under an atmosphere of dried and deoxygenated nitrogen or argon with standard Schlenk techniques.[8a,31] Solvents were refluxed over and then distilled from appropriate drying agents under N_2 prior to use (hexane, benzene, toluene, diethyl ether, diisopropyl ether, tetrahydrofuran, and dioxane from sodium benzophenone ketyl; dichloromethane from P_2O_5; acetonitrile from P_2O_5 and then from K_2CO_3). 1,5-Cyclooctadiene was dried over and vacuum-distilled from CaH_2. Olefins were dried over appropriate drying agents and vacuum-distilled prior to use. Maleic anhydride, concentrated sulfuric acid, iodine, and carbon monoxide were used as purchased. Tertiary phosphines and phosphite used in this study were prepared by the literature methods.[32] Infrared spectra were measured on a Jasco IR A302 and an FTIR 5M spectrometers. ^1H and $^{13}C\{^1H\}$ NMR spectra were obtained on JEOL FX-200 (^1H, 199.5 MHz) and GX-400 (^{13}C, 100.4 Hz) spectrometers by using ^1H (of residual protons) and ^{13}C NMR signals of deuteriated solvents as internal references [C_6D_6 (^1H, δ 7.15), $CDCl_3$ (^1H, δ 7.25; ^{13}C, δ 77.0). NMR solvents were freeze-pump-thaw degassed three times and then vacuum transferred from appropriate drying agents (C_6D_6 from Na; $CDCl_3$ from P_2O_5). UV-vis spectra were obtained on a Hitachi 320A and a Shimadzu UV-120-02 spectrophotometers. Elemental analyses were performed with a Yanagimoto CHN Autocorder MT-2. Molar electric conductivities were measured by a TOA Conduct Meter CM-5B. Gases were quantitatively analyzed by gas chromatography (Shimadzu GC-8AFP, GC-3BT) using the internal standard method, and in some cases a Toepler pump was used to measure the total volume of evolved gases. Liquids formed in reactions were analyzed by GC.

The starting materials and related complexes were prepared by the literature methods with minor modifications: PtMeCl(cod),[33] PtEtCl(cod),[34] PtPhCl(cod),[33] Pt(2-MeC_6H_4)Cl(cod),[33] Pt(4-MeC_6H_4)Cl(cod),[33] Pt(2,6-$(Me)_2C_6H_3$)I(cod),[33] Pt(4-$MeOC_6H_4$)Cl(cod),[33] Pt(C_6F_5)I(cod),[33] Pt(4-FC_6H_4)Cl(cod),[33] Pt(4-ClC_6H_4)Cl(cod),[33] Na[$WCp(CO)_3$],[35] Na[$W(C_5H_4Me)(CO)_3$],[36] Na[$W(C_5H_4COOMe)(CO)_3$],[36] Na[$MoCp(CO)_3$],[35] PtMeI(cod),[33] $WCp(CO)_3I$,[37] PtI_2(cod),[38] $PtMeI(PPh_3)_2$.[39]

Products of the organic group migration (Table 5) were characterized by comparing their ^1H NMR data to those of authentic W and Mo complexes prepared by the literature method, *e.g.*, $MeWCp(CO)_3$,[35] $EtWCp(CO)_3$,[35] $PhWCp(CO)_3$,[40] $MeMoCp(CO)_3$.[35]

Synthesis of Heterodinuclear Complexes. A typical procedure for (cod)MePt−$WCp(CO)_3$ (**1a**) is given. A Schlenk flask was charged with PtMeCl(cod) (57.7 mg, 0.162 mmol) and Na[$WCp(CO)_3$] (58.8 mg, 0.165 mmol). THF (10 mL) was added at 0 °C and the solution was stirred for 2 h to give a dark red solution. The solution was evaporated to dryness and the resulting red-brown solids were extracted with benzene. After the filtered solution was again evaporated to dryness, the red solids were extracted with THF and addition of hexane gave red needles. The crystals were washed with cold hexane and dried under vacuum at 0 °C (77.6 mg). Yield: 73%. Mp: 105 °C dec. Anal. Calcd for $C_{17}H_{20}O_3WPt$: C, 31.30; H, 3.16. Found: C, 31.35; H, 3.16. Molar electric conductivity Λ (in THF at rt): 0.02 S cm^2 mol^{-1}. IR (ν_{CO}, KBr): 1894, 1795 cm^{-1}. UV-vis (THF): 285 nm ($\epsilon = 6.00 \times 10^4$ M^{-1} cm^{-1}).

^1H NMR data of the new heterodinuclear complexes **1a**−**4c** are summarized in Table 1. Complexes **1d**, **1f**, **1h**, **2a**, **2b**, **3a**, and **3b** were synthesized by a similar method to that for **1a** except that nitrato complexes $PtR(NO_3)$(cod) prepared *in situ* from PtRX(cod) and $AgNO_3$ were used instead.

(cod)EtPt−$WCp(CO)_3$ (**1b**): red-purple needles from CH_2Cl_2/hexane. Yield: 40%. Mp: 52 °C dec. Anal. Calcd for $C_{18}H_{22}O_3WPt$: C, 32.50; H, 3.33. Found: C, 32.49; H, 3.64. IR (ν_{CO}, KBr): 1897, 1793 cm^{-1}. UV-vis (THF): 284 nm ($\epsilon = 1.69 \times 10^4$ M^{-1} cm^{-1}).

(cod)PhPt−$WCp(CO)_3$ (**1c**): red needles from CH_2Cl_2/hexane. Yield: 45%. Mp: 129 °C dec. Anal. Calcd for $C_{22}H_{22}O_3WPt$: C, 37.40; H, 3.11. Found: C, 37.17; H, 3.12. IR (ν_{CO}, KBr): 1902, 1805 cm^{-1}. UV-vis (THF): 296 nm ($\epsilon = 1.60 \times 10^4$ M^{-1} cm^{-1}).

(cod) (2-MeC_6H_4)Pt−$WCp(CO)_3$ (**1d**): red plates from CH_2Cl_2/hexane. Yield: 37%. Mp: 140−142 °C dec. Anal. Calcd for $C_{23}H_{24}O_3WPt$: C, 37.98; H, 3.33. Found: C, 37.45; H, 3.27. IR (ν_{CO}, KBr): 1910, 1807 cm^{-1}. UV-vis (THF): 299 nm ($\epsilon = 3.21 \times 10^4$ M^{-1} cm^{-1}). $^{13}C\{^1H\}$ NMR ($CDCl_3$, rt) δ 226.0 (s,

(31) Shriver, D. F.; Drezdzon, M. A. *The Manipulation of Air-Sensitive Compounds*; 2nd ed.; Wiley: New York, 1986.
(32) Kosolapoff, G. M.; Maier, L. *Organic Phosphorus Compounds*; Wiley: New York, 1972; Vol. 1, and references therein.
(33) Clark, H. C.; Manzer, L. E. *J. Organomet. Chem.* **1973**, *59*, 411.
(34) Clark, H. C.; Manzer, L. E. *J. Organomet. Chem.* **1971**, *33*, 241.
(35) Piper, T. S.; Wilkinson, G. *J. Inorg. Nucl. Chem.* **1956**, *3*, 104.
(36) Hart, W. P.; Macomber, D. W.; Rausch, M. D. *J. Am. Chem. Soc.* **1980**, *102*, 1196.
(37) Sloan, T. E.; Wojcicki, A. *Inorg. Chem.* **1968**, *7*, 1268.
(38) McDermott, J. X.; White, J. F.; Whitesides, G. M. *J. Am. Chem. Soc.* **1976**, *98*, 6521.
(39) Chatt, J.; Shaw, B. L. *J. Chem. Soc.* **1959**, 705.
(40) Mahmond, K. A.; Rest, A. J.; Alt, H. G.; Eichmer, M. E.; Jansen, B. M. *J. Chem. Soc., Dalton Trans.* **1984**, 175.

CO), 223.5 (s, CO), 222.7 (s, CO), 141.1 (s, 2-MeC_6H_4 *ipso* bearing Me or Pt), 137.3 (s, 2-MeC_6H_4 *ipso* bearing Me or Pt), 135.0 (s, 2-MeC_6H_4 arom *C*H), 129.5 (s, J_{PtC} = 45 Hz, 2-MeC_6H_4 arom *C*H), 125.1 (s, J_{PtC} = 57 Hz, 2-MeC_6H_4 arom *C*H), 123.2 (s, 2-MeC_6H_4 arom *C*H), 119.0 (s, J_{PtC} = 27 Hz, olefinic, cod =*C*H *cis* to W), 118.2 (s, J_{PtC} = 33 Hz, olefinic, cod =*C*H *cis* to W), 103.6 (s, J_{PtC} = 115 Hz, olefinic, cod =*C*H *trans* to W), 99.7 (s, J_{PtC} = 108 Hz, olefinic, cod =*C*H *trans* to W), 91.1 (s, Cp), 32.7 (s, cod CH_2 *cis* to W), 30.5 (s, J_{PtC} = 20 Hz, cod CH_2 *cis* to W), 29.8 (s, cod CH_2 *trans* to W), 28.2 (s, cod CH_2 *trans* to W), 25.8 (s, J_{PtC} = 51 Hz, 2-*Me*C_6H_4).

(cod)(4-MeC_6H_4)Pt–$WCp(CO)_3$ (**1e**): red needles from THF/hexane. Yield: 37%. Mp: 110 °C dec. Anal. Calcd for $C_{23}H_{24}O_3WPt$: C, 37.98; H, 3.33. Found: C, 37.77; H, 3.12. IR (ν_{CO}, KBr): 1901, 1811 cm^{-1}. UV-vis (THF): 298 nm.

(cod)(2,6-$(Me)_2C_6H_3$)Pt–$WCp(CO)_3$ (**1f**): red needles from THF/hexane. Yield: 31%. Mp: 146 °C dec. This complex was identified by the spectroscopic methods. IR (ν_{CO}, KBr): 1930, 1843, 1821 cm^{-1}. UV-vis (THF): 301 nm.

(cod)(4-$MeOC_6H_4$)Pt–$WCp(CO)_3$ (**1g**): red plates from THF/hexane. Yield: 27%. Mp: 105 °C dec. This complex was identified by the spectroscopic methods. IR (ν_{CO}, KBr): 1897, 1794 cm^{-1}. UV-vis (THF): 298 nm.

(cod)(C_6F_5)Pt–$WCp(CO)_3$ (**1h**): deep-red needles from THF/hexane. Yield: 10%. Mp: 148 °C dec. Anal. Calcd for $C_{22}H_{17}O_3F_5WPt$: C, 32.89; H, 2.13. Found: C, 32.59; H, 2.22. IR (ν_{CO}, KBr): 1933, 1836 cm^{-1}. UV-vis (THF): 303 nm.

(cod)(4-FC_6H_4)Pt–$WCp(CO)_3$ (**1i**): red plates from THF/hexane. Yield: 42%. Mp: 138 °C dec. Anal. Calcd for $C_{22}H_{21}O_3FWPt$: C, 36.13; H, 2.89. Found: C, 35.56; H, 3.13. IR (ν_{CO}, KBr): 1907, 1804 cm^{-1}. UV-vis (THF): 296 nm.

(cod)(4-ClC_6H_4)Pt–$WCp(CO)_3$ (**1j**): red needles from THF/hexane. Yield: 52%. This complex was identified by the spectroscopic methods. IR (ν_{CO}, KBr): 1904, 1809 cm^{-1}. UV-vis(THF): 297 nm.

(cod)MePt–$W(C_5H_4Me)(CO)_3$ (**2a**): red needles from THF/hexane. Yield: 34%. Mp: 102 °C dec. Anal. Calcd for $C_{18}H_{22}O_3WPt$: C, 32.50; H, 3.33. Found: C, 32.52; H, 3.37. Λ (in THF at rt): 0.0053 S cm^2 mol^{-1}. IR (ν_{CO}, KBr): 1892, 1780 cm^{-1}. UV-vis (THF): 285 nm.

(cod)PhPt–$W(C_5H_4Me)(CO)_3$ (**2b**): red plates from THF/hexane. Yield: 60%. Mp: 118 °C dec. Anal. Calcd for $C_{23}H_{24}O_3WPt$: C, 37.98; H, 3.33. Found: C, 37.74; H, 3.24. Λ (in THF at rt): 0.00031 S cm^2 mol^{-1}. IR (ν_{CO}, KBr): 1903, 1798 cm^{-1}. UV-vis (THF): 298 nm.

(cod)MePt–$W(C_5H_4COOMe)(CO)_3$ (**3a**): red needles from THF/hexane. Yield: 26%. Mp: 117 °C dec. Anal. Calcd for $C_{19}H_{22}O_5WPt$: C, 32.17; H, 3.13. Found: C, 32.50; H, 3.19. Λ (in THF at rt): 0.012 S cm^2 mol^{-1}. IR (ν_{CO}, KBr): 1918, 1836, 1803 cm^{-1}. UV-vis (THF): 289 nm.

(cod)PhPt–$W(C_5H_4COOMe)(CO)_3$ (**3b**): red needles from THF/hexane. Yield: 20%. Mp: 123 °C dec. Λ (in THF at rt): 0.0013 S cm^2 mol^{-1}. This complex was identified by the spectroscopic methods. IR (ν_{CO}, KBr): 1904, 1818, 1802 cm^{-1}. UV-vis (THF): 298 nm.

(cod)MePt–$MoCp(CO)_3$ (**4a**): deep-red needles from CH_2Cl_2/hexane. Yield: 44%. Mp: 116 °C dec. Anal. Calcd for $C_{17}H_{20}O_3MoPt$: C, 36.24; H, 3.58. Found: C, 36.25; H, 3.58. Λ (in THF at rt): 0.02 S cm^2 mol^{-1}. IR (ν_{CO}, KBr): 1899, 1802 cm^{-1}. UV-vis (THF): 283 nm.

(cod)PhPt–$MoCp(CO)_3$ (**4b**): deep-red cubic crystals from CH_2Cl_2/hexane. Yield: 30%. Mp: 133 °C dec. Anal. Calcd for $C_{22}H_{22}O_3MoPt$: C, 42.25; H, 3.55. Found: C, 42.05; H, 3.46. IR (ν_{CO}, KBr): 1905, 1810 cm^{-1}. UV-vis (THF): 298 nm.

(cod)(2-MeC_6H_4)Pt–$MoCp(CO)_3$ (**4c**): red-brown cubic crystal from CH_2Cl_2/hexane. Yield: 33%. Mp: 165 °C dec. Anal. Calcd for $C_{23}H_{24}O_3MoPt$: C, 43.20; H, 3.78. Found: C, 42.59; H, 3.90. Λ (in THF at rt): 0.05 S cm^2 mol^{-1}. IR (ν_{CO}, KBr): 1915, 1813 cm^{-1}. UV-vis (THF): 303 nm.

Acidolysis of 1a and 4a. Typically, **4a** (21.0 mg, 0.037 mmol) was placed in a Schlenk flask with a serum cap and degassed. Sulfuric acid (100 μL) was added by a hypodermic syringe. After 1 h of stirring at room temperature, methane (91%) was detected by GC (column: Porapak Q, 2 m). Similar reaction of **1a** gave methane in 97% yield.

Iodination of 1a. An NMR sample tube containing **1a** (11.0 mg, 0.017 mmol) and I_2 (0.039 mmol) was attached to a vacuum line, and dry C_6D_6 (0.4 mL) was introduced by vacuum transfer. After the tube was sealed, the system was allowed to stand at room temperature for 30 min. ^1H NMR revealed the complete consumption of **1a** and the formation of PtMeI(cod) (54%) and $WCp(CO)_3I$ (46%). After further standing of the system for 3.5 h, the signals of PtMeI(cod) completely disappeared but those of $WCp(CO)_3I$ (66%) and MeI (66%) were observed.

X-ray Diffraction Study of 4b. A crystal of **4b** sealed in a thin-glass capillary under N_2 was mounted on a Rigaku automated four-circle diffractometer. Accurate unit-cell parameters were determined by the least-squares fit of 2θ values of 25 strong reflections. Intensity data collection was carried out using Mo Kα radiation by the $\theta-2\theta$ scan mode. The scan speed and range were 4° min^{-1} in 2θ and $\Delta(2\theta) = 2.0 + 0.7 \tan\theta$, respectively. The background intensities were measured for 5 s at both ends of a scan. A total of 4433 independent reflections (R_{int} = 0.020) were collected with $\sin\theta/\lambda$ up to 0.64. Absorption correction was applied to the intensity data.[41] The minimum normalized transmission factor which was based on intensities obtained by the azimuthal scan of 202 reflection was 0.11. The crystal is isomorphous with that of the Pt–W analogue **1c**.[7] The atomic coordinates of **1c** were employed as a starting model of **4b**. The structure was solved by the heavy metal method and refined by the block-diagonal least-squares procedure using HBLS-V.[42] Non-hydrogen atoms were refined anisotropically except for the C(1), C(20), and O(1) atoms which were refined with the isotropic thermal parameters. All the hydrogen atoms whose positions were estimated from stereochemical consideration were included in the structure factor calculation. At the final stages of refinement, two reflections (200 and 002) were excluded due to extinction effects. The final R and R_w values are 0.057 and 0.078 for 3719 [$|F_o| > 3\sigma(|F_o|)$] reflections, respectively. The weighting scheme used in the final refinement cycles is $w = (\sigma_{cs}^2 + 0.015|F_o| + 0.002|F_o|^2)^{-1}$. The atomic scattering factors were taken from the International Tables for X-ray Crystallography.[43] The final atomic parameters are listed in supplementary material. Computations were done on an ACOS 930 computer at the Research Center for Protein Engineering, Institute for Protein Research, Osaka University, Japan.

Thermolysis of Heterodinuclear Complexes. The thermolysis reactions were carried out in Schlenk flasks. Typically, a C_6D_6 solution of **1a** (15.6 mg, 0.024 mmol) was placed in a Schlenk flask with a serum cap and degassed. After 2 h of stirring at 70 °C, the flask was cooled to room temperature. *n*-Butane (1.23 mL) was added as an internal standard and evolved gas was analyzed by GC: CH_4 (6%). To the resulting solution was added dioxane (1.0 μL) as an internal standard, and the product was quantitatively analyzed by ^1H NMR ($MeWCp(CO)_3$, 73%). For other complexes having aryl groups on Pt, the thermolysis was carried out in an NMR tube under the same conditions, and the products and yields were analyzed by ^1H NMR (Table 5).

The reaction to characterize Pt products in the thermolysis of **1a** was carried out as follows: to a Schlenk flask containing **1a** (25.0 mg, 0.038 mmol) and PPh_3 (44.9 mg, 0.171 mmol) was added benzene (1 mL) at room temperature. The solution was stirred for 4 h to give an orange solution. MeI (100 μL, 0.162

(41) North, A. C. T.; Phillips, D. C.; Matthews, B. W. *Acta Crystallogr. Sect. A* **1968**, *24*, 351.
(42) Ashida, T. *HBLS-V, The Universal Crystallographic Computing System-Osaka*; The Computation Center, Osaka Univ.: Osaka, Japan, 1979, p 53.
(43) Cromer, D. T.; Waber, J. T. *International Tables for X-ray Crystallography*; Kynoch Press: Birmingham, U.K., 1974; Vol. IV, p 71.

mmol) was added to the solution and the mixture was stirred for 1 day to give a red-brown solution containing white precipitates. The solution was filtered and evaporated to dryness, and then the resulting red-brown solids were extracted with $CDCl_3$. The ^1H NMR showed the formation of $PtMeI(PPh_3)_2$ (25%).

A crossover experiment in the thermolysis of **1d** and **2b** was carried out as follows: a C_6D_6 (0.35 mL) solution of **1d** (9.6 mg, 0.013 mmol) and **2b** (11.3 mg, 0.016 mmol) was placed in an NMR sample tube. Dioxane (1.0 μL) was added to the solution, and the sample tube was heated to 70 °C. After 15 min the tube was cooled to room temperature, and the ^1H NMR was measured. Heating the sample at 70 °C and the NMR measurement were repeated by the total reaction time of 45 and 120 min. $(2\text{-}MeC_6H_4)WCp(CO)_3$ (**9**) and $PhW(C_5H_4Me)(CO)_3$ (**10**) were observed as products. The reaction time and respective yields of **9** and **10** based on **1d** and **2b** are as follows: 15 min, **9**: 15%, **10**: 30%; 45 min, **9**: 20%, **10**: 41%; 120 min, **9**: 28%, **10**: 43%.

Effect of Carbon Monoxide. The procedure for **1b** is given. A solution of **1b** (26.0 mg, 0.039 mmol) in C_6D_6 (0.4 mL) was placed in a Schlenk flask equipped with a serum cap. The flask was degassed and CO gas (1 atm) was introduced. After stirring at room temperature for 2 h, *n*-butane (1.23 mL) was added as an internal standard and evolved gases were analyzed by GC: C_2H_4 (37%), C_2H_6 (20%). After addition of dioxane (1.0 μL), the solution was transferred to an NMR sample tube and the ^1H NMR spectrum showed formation of $EtWCp(CO)_3$ (13%). Reactions of **1a**, **1c**, and **4a** with CO were similarly examined and the corresponding products (yields) were CH_4 (trace) and $MeWCp(CO)_3$ (73%) from **1a**, $PhWCp(CO)_3$ (72%) from **1c**, and $MeMoCp(CO)_3$ (45% in 4 h of reaction time) from **4a**.

To characterize Pt products in the reaction of **1a** with CO, the following reaction was performed: a Schlenk flask containing **1a** (26.2 mg, 0.040 mmol) and THF (1 mL) was evacuated and CO (1 atm) was introduced. The red solution was stirred at −30 °C for 4 h to give a green solution. When PPh_3 (21.9 mg, 0.083 mmol) was added, the solution turned red and finally yellow in 1 h of stirring. The solution was evaporated to dryness and an IR spectrum of the resulting yellow solid in Nujol indicated the presence of $Pt(CO)_2(PPh_3)_2$ (ν_{CO}: 1982, 1945 cm^{-1}) and $Pt(CO)(PPh_3)_3$ (1907 cm^{-1}).[13]

Effect of Tertiary Phosphines. An NMR sample tube containing **1a** (10 mg, 0.015 mmol) was attached to a vacuum line, and dry C_6D_6 (0.4 mL) was introduced by vacuum transfer. After 15-fold excess tertiary phosphines (10−30 μL) and dioxane (1.0 μL) were added to the solution, the system was allowed to stand at room temperature for 2 h. Yields of $MeWCp(CO)_3$ were determined by ^1H NMR.

The procedure to isolate $[Pt(PMe_3)_3Me]^+[WCp(CO)_3]^-$ (**5**) is as follows: to a Schlenk flask containing **1a** (72.4 mg, 0.111 mmol) and benzene (1 mL) was added PMe_3 (34 μL, 0.33 mmol) at room temperature. The original red solution immediately gave a colorless solution and white precipitates, and the mixture was stirred for 1 h. After filtration of the mixture, the precipitates were washed with hexane and dried under vacuum. Extraction with CH_2Cl_2 and addition of hexane gave yellow cubic crystals of **5**. Yield: 33%. Mp: 145 °C dec. Anal. Calcd for $C_{18}H_{35}O_3P_3WPt$: C, 28.03; H, 4.57. Found: C, 27.97; H, 4.55. Λ (THF, rt) 6.8 S cm^2 mol^{-1}. IR (ν_{CO}, KBr): 1882, 1758 cm^{-1}. ^1H NMR ($CDCl_3$, rt) δ 0.42 (d, 3H, J_{PH} = 6.4 Hz, J_{PtH} = 57.3 Hz, PtMe), 1.74 (d, 3H, J_{PH} = 8.6 Hz, J_{PtH} = 18.8 Hz, PMe_3), 1.65 (br, 6H, PMe_3), 5.23 (s, 5H, WCp).

Effect of Substituted Olefins. The procedure for **1a** is given. An NMR sample tube containing **1a** (10 mg, 0.015 mmol) was attached to a vacuum line, and dry C_6D_6 (0.4 mL) was introduced by vacuum transfer. After 15-fold excess olefin and dioxane (1.0 μL) were added to the solution, the system was allowed to stand at room temperature for 2 h. Products were analyzed by ^1H NMR and the yields of $MeWCp(CO)_3$ in adding each olefin were as follows: maleic anhydride, 37%; acrylonitrile, 13%; methacrylonitrile, trace; methyl acrylate, trace; *trans*-stilbene, trace; vinyl acetate, trace. Similarly, the yields of $PhWCp(CO)_3$ from the reaction of **1c** with olefins were as follows: maleic anhydride, trace; acrylonitrile, 16%; methacrylonitrile, trace; methyl acrylate, trace; *trans*-stilbene, trace; vinyl acetate, trace.

Kinetic Study of the Organic Group Migration. The procedure for the methyl migration for **1a** in the presence of AN is given. An optical cell attached to a Schlenk flask was used for measurement of UV-vis spectra under an atmosphere of N_2.[44] To the Schlenk flask containing **1a** (0.002 mmol) was introduced dry THF (5−8 mL) by vacuum transfer, and the volume of added THF was estimated from the weight. A known amount of AN (10−500 μL) was added to the solution by a hypodermic syringe, and the concentration of AN was precisely calculated. The temperature of the cell was kept constant at 38 ± 1 °C using a Yamato CTE-310 or an EYELA NCB-110 circulator. The reaction was monitored by electronic absorption spectra in 250−330 nm (Figure 2), and the decrease in absorbance of the peak at 285 nm was used to calculate $\ln([Pt]_0/([Pt]_0 - [\mathbf{8}])$. First order plot of $\ln([Pt]_0/([Pt]_0 - [\mathbf{8}])$ versus time gave a straight line (Figure 3), and a pseudo-first order rate constant was estimated from the slope: $k_{obsd} = 1.12 \times 10^{-4}$ S^{-1}.

Supplementary Material Available: For the organic group migration reactions, tables of k_{obsd} corresponding to Figures 5, 7, 10, and 11; for the X-ray crystallography of **4b**, tables of atomic coordinates of H atoms, anisotropic temperature factors of non-H atoms, and bond distances and bond angles of non-H atoms (8 pages). Ordering information is given on any current masthead page.

OM940004A

(44) Reference 8a, p 169.